Atmos. Chem. Phys. Discuss., 7, 5365–5412, 2007
www.atmos-chem-phys-discuss.net/7/5365/2007/

Atmospheric Chemistry and Physics Discussions

Oxidative capacity of the Mexico City atmosphere – Part 1: A radical source perspective

R. Volkamer[1,2], **P. M. Sheehy**[1,3], **L. T. Molina**[1,3], **and M. J. Molina**[2]

[1]Department of Earth, Atmospheric and Planetary Sciences, Massachussetts Institute of Technology, Cambridge, MA, USA
[2]Department of Chemistry and Biochemistry, University of California, San Diego, La Jolla, CA, USA
[3]Molina Center for Energy and the Environment (MCE[2]), La Jolla, CA, USA

Received: 27 March 2007 – Accepted: 3 April 2007 – Published: 19 April 2007

Correspondence to: R. Volkamer (rainer@alum.mit.edu)

Abstract

A detailed analysis of OH, HO_2 and RO_2 radical sources is presented for the near field photochemical regime inside the Mexico City Metropolitan Area (MCMA). During spring of 2003 (MCMA-2003 field campaign) an extensive set of measurements was collected to quantify time resolved RO_x (sum of OH, HO_2, RO_2) radical production rates from day- and nighttime radical sources. The Master Chemical Mechanism (MCMv3.1) was constrained by measurements of (1) concentration time-profiles of photosensitive radical precursors, i.e., nitrous acid (HONO), formaldehyde (HCHO), ozone (O_3), glyoxal (CHOCHO), and other oxygenated volatile organic compounds (OVOCs); (2) respective photolysis-frequencies (J-values); (3) concentration time-profiles of alkanes, alkenes, and aromatic VOCs (103 compound are treated) and oxidants, i.e., OH- and NO_3 radicals, O_3; and (4) NO, NO_2, meteorological and other parameters. The RO_x production rate was calculated directly from these observations; MCM was used to estimate further RO_x production from unconstrained sources, and express overall RO_x production as OH-equivalents (i.e., taking into account the propagation efficiencies of RO_2 and HO_2 radicals into OH radicals).

Daytime radical production is found to be about 10-25 times higher than at night; it does not track the abundance of sunlight. 12-h average daytime contributions of individual sources are: HCHO and O_3 photolysis, each about 20%; O_3/alkene reactions and HONO photolysis, each about 15%; unmeasured sources about 30%. While the direct contribution of O_3/alkene reactions appears to be moderately small, source-apportionment of ambient HCHO and HONO identifies O_3/alkene reactions as being largely responsible for jump-starting photochemistry about one hour after sunrise. The peak radical production is found to be higher than in any other urban influenced environment studied to date; further, differences exist in the timing of radical production.

Our measurements and analysis comprise a database that enables testing of the representation of radical sources in photochemical models. Since the photochemical processing of pollutants is radical-limited in the MCMA, our analysis identifies the

drivers for such processing. Three pathways are identified by which reductions in VOC emissions induce reductions in peak concentrations of secondary pollutants, such as O_3 and secondary organic aerosol (SOA).

1 Introduction

Air pollution is an increasingly important concern in the public health debate (Health Effects Institute, 2000). In Mexico City the number of deaths associated with anthropogenic air pollution is comparable to that from car accidents (Molina and Molina, 2002). Ozone (O_3) and fine particulate matter ($PM_{2.5}$, particles with a diameter smaller than 2.5 micrometers) are integral components of photochemical smog. There is no evidence of a "threshold" for O_3 or $PM_{2.5}$ related health effects. O_3 is known to cause inflammation in the respiratory tract, reduce respiratory capacity for some people, and increase hospitalization rates related to asthma and other respiratory ailments. More recently, systematic evidence has been presented supporting premature mortality in relation to short-term O_3 exposure following episodes of photochemical smog in the US (Bell et al., 2004) and Asia (PAPA, 2004). Short term exposures to high levels of $PM_{2.5}$ (e.g., 500 $\mu g/m^3$) caused premature mortality during the London killer smog episode in 1952 (Davis et al., 2002); more recent studies in the U.S., Europe, Asia, and South America have further found association of long-term exposures to $PM_{2.5}$ with premature mortality at much lower levels (<50 $\mu g/m^3$) (Health Effects Institute, 2000; Pope et al., 2002). Recent progress toward identifying biological mechanisms for these effects point to the role of transition metals and pro-oxidative hydrocarbons associated with fine particulate matter (Nel, 2005). Downwind of urban areas, photochemical O_3 leads to reduced tree-growth (Gregg et al., 2003), has adverse effects on agriculture (Fuhrer and Booker, 2003), and contributes to global warming (IPCC, 2007). Enhanced light absorption by aerosols affects climate (Ramanathan et al., 2001) with implications for atmospheric stability and vertical air exchange, precipitation patterns, and the amount of radiation reaching the ground.

Photochemical smog is largely formed as the result of the chemical transformations of primary emissions to the atmosphere. For O_3 this has long been understood (Hagen-Smith et al., 1951). On the other hand, it has only recently been recognized that in Mexico City – despite the abundance of emission sources – gas-to-particle conversion processes are responsible for about 70–80% of $PM_{2.5}$ mass (Salcedo et al., 2006); secondary organic aerosol (SOA) originating from the gas-phase oxidation of hydrocarbons is a major component of $PM_{2.5}$ in the afternoon (Volkamer et al., 2006). Free radical (i.e., OH and NO_3), O_3, and photolysis reactions initiate the oxidation of hydrocarbons in the gas-phase, and possibly modify aerosol surfaces. The design of effective policy strategies to reduce the impact of air pollution on human health, ecosystem and climate requires understanding the sources and sinks of these radicals. Modeling studies (Ruiz-Suarez et al., 1993; West et al., 2004; Lei et al., 2006) and experimental observations (Arriaga-Colina et al., 2004) suggest that the photochemical processing of pollutants in the MCMA is either VOC limited or suppressed by high NO_x levels; indeed both of these chemical regimes may apply at different times of the same day (Lei et al., 2006; Madronich, personal communication). In either case, the photochemical processing of pollutants is radical-limited. This suggests that a more detailed understanding of radical sources can identify mechanisms to efficiently slow down photochemical smog formation, including O_3 and SOA formation in the MCMA.

In this paper we quantify time resolved production of OH, HO_2 and RO_2 radicals (in sum termed RO_x radicals) from the reaction of closed shell molecules (i.e., HONO, HCHO, O_3, glyoxal, numerous other oxygenated VOC (OVOC)) with sunlight, and the dark reaction of alkenes with O_3 and NO_3 radicals. For HONO and HCHO, two important radical precursors, a source apportionment analysis is presented. In a companion paper (Sheehy et al., 2007[1]) the experimental radical production rates from this work are combined with observations of HO_x radicals to assess current capabilities to pre-

[1]Sheehy, P., Volkamer, R., Molina, L. T., Molina, M. J.: Oxidative Capacity of the Mexico City atmosphere. Part 2: A ROx radical cycling perspective, Atmos. Chem. Phys. Discuss., submitted, 2007.

dict the oxidation capacity of Mexico City air in light of existing gaps in our mechanistic understanding of hydrocarbon oxidation (Carter, 2005; Bloss et al., 2005a, b).

2 Experimental

As part of a field campaign in the Mexico City Metropolitan Area (MCMA) during spring of 2003 (MCMA-2003), time-resolved production of HO_x radicals released from the decomposition of closed shell molecules were quantified. A comprehensive set of instrumentation to characterize radical precursor concentrations, their respective photolysis frequencies, and oxidants (OH, O_3, NO_3) was based at a supersite located at the Centro Nacional de Investigación y Capacitación Ambiental (CENICA) in the central-southern part of the MCMA.

2.1 Measurement techniques

Two long-path Differential Optical Absorption Spectrometry (LP-DOAS) instruments were deployed on the roof-top of the CENICA building. DOAS uses unique specific narrow-band (<5 nm) absorption structures in the visible spectral range to separate trace gas absorptions from broadband molecule and aerosol extinction in the open atmosphere (Platt, 1994). The DOAS#1 light path was directed towards an antenna tower in a south-easterly direction at an average height of 16 m with a 430 m path length (total 860 m). DOAS#2 faced an array of retroreflectors at Museo Fuego Nuevo (Cerro de la Estrella) resulting in a total atmospheric light-path of 4420 m on average 70 m above ground. Atmospheric spectra were recorded by sequentially projecting 40-nm (DOAS#1) and 80-nm (DOAS#2) wide wavelength intervals centered around 260 nm, 318 nm, 357 nm, 427 nm and 642 nm onto the 1024-element linear photodiode array detector; background spectra recorded within a few minutes were subtracted to correct for stray-light from the atmosphere. The average time-resolution for a full cycle of spectra ranged between 2–15 min.

From the spectra collected by DOAS#1, ozone was evaluated in the wavelength range between 252 and 262 nm, using non-linear least squares fitting of two oxygen reference spectra, two O_3 references at 293 K and 313 K, numerous aromatic hydrocarbons, following the procedure developed by Volkamer et al. (1998). From the spectra collected by DOAS#2, HCHO and ozone were evaluated in the wavelength range between 324 to 358 nm using non-linear least squares fitting of HCHO, HONO, NO_2, two O_3 references at 293 K and 313 K, SO_2, and a 5th order polynomial high pass filter. HONO was retrieved in the wavelength range between 321 to 372 nm using non-linear least squares fitting of HONO, HCHO, NO_2, two O_3 references at 293 K and 313 K, SO_2, and a 9th order polynomial high-pass filter. Glyoxal was retrieved from the evaluation of the spectral range between 420 and 465 nm, using non-linear least squares fitting of CHOCHO, NO_2, O_4, H_2O, two lamp-reference spectra, and a 5th order polynomial high-pass filter; these data are discussed in more detail by Volkamer et al. (2005a). In addition, NO_3 radicals were detected at nighttime. Reference spectra were calculated from high-resolution absorption cross-section spectra, which were degraded to our instrument resolution (ca. 0.4 nm FWHM), and fitted using the Windoas and MFC software packages (Gomer et al., 1993; Fayt and van Roozendael, 2001). The trace-gas concentrations reported here rely on the following calibrations, with values in parentheses indicating mean detection limits: HONO (190 pptv) (Stutz et al., 2000), CHOCHO (150 pptv) (Volkamer et al., 2005b), NO_3 (5 pptv) (Sander et al., 2006), O_3 (DOAS#1: 1.3 ppbv; DOAS#2: 5 ppbv) (Bass and Paur, 1981), and SO_2 (150 pptv) (Vandaele et al., 1994). For HCHO (1 ppbv) the cross-section by Cantrell et al. (1990) was used for spectra evaluation; the concentrations were multiplied by 1.22 to reflect the results from cross-calibration of ultraviolet and infrared spectral parameters of HCHO (Volkamer et al., 2002[2]). For NO_2 (430 pptv), reference spectra were recorded by placing a 2-cm long quartz-cuvet into the light beam, which was filled previously with a mixture of approximately 1% NO_2/N_2 to atmospheric pressure. The $HONO/NO_2$ ratio was determined from simultaneous fitting of resolution-adjusted

[2]Volkamer et al., 2002, CP26 at http://checfs2.ucsd.edu/~rainer/publications/index.html

literature cross-sections and any HONO contamination of the cuvet was corrected by subtracting an appropriately scaled HONO spectrum from the cuvet spectrum. This approach eliminates the possibility of HONO contaminated NO_2 reference spectra; we successfully used it in cross-comparisons of the DOAS and LOPAP techniques (Kleffmann et al., 2006). NO_2 concentrations were scaled to match the average of various NO_2 reference spectra as determined by Orphal (2003). Trace-gas concentrations that were evaluated in different spectral ranges (HONO, NO_2, HCHO and O_3) were found to be independent of the spectral range used for evaluation (within error limits). The above listed wavelength intervals reflect smallest overall uncertainties with the measurements.

Acetaldehyde (CH_3CHO) and acetone (CH_3COCH_3) were measured by a Proton-Transfer-Reaction Mass-Spectrometer (PTR-MS) (Jobson et al., 2007[3]), which was co-located with the DOAS instruments at CENICA roof-top, about 16 m above the ground. The PTR-MS sensitivity was determined with a multi-component compressed gas standard from Apel-Reimer Environmental (Denver, USA) containing acetaldehyde and acetone, among other hydrocarbons. The standard had a stated accuracy of ±5% for oxygenated species, better than 5% for hydrocarbons, and multipoint calibrations were performed every couple of days. Additional measurements of alkenes by a Fast Isoprene Sensor (FIS), supplemented by gas-chromatography (GC-FID) analysis of canister samples are described in detail elsewhere (Velasco et al., 2007).

Photolysis frequencies of HONO (J_{HONO}), HCHO (J_{HCHO}), CH_3CHO (J_{CH3CHO}), O_3 (J_{O3}), CHOCHO (J_{CHOCHO}), CH_3COCH_3 ($J_{CH3COCH3}$) and other trace gases were measured by spectroradiometry. The spectroradiometer was mounted on top of the measurement cabin with a clear field of view and measured solar actinic flux spectra from 280 nm to 450 nm with a spectral band pass of 1 nm. The step width was set to 2 nm below 320 nm, and 5 nm above. The radiation from the upper hemisphere was collected

[3]Jobson, B. T., Alexander, M. L., Prazeller, P., et al.: Intercomparison of Volatile Organic Carbon Measurements Techniques and Data from the MCMA 2003 Field Experiment, Atmos. Chem. Phys. Discuss., in preparation, 2007.

by a diffuser-optic with almost uniform sensitivity for all angles of incidence within a solid angle of 2πsr. A double monochromator (Bentham DMc 150) equipped with a tunable grating (2400 grooves/mm) was used for wavelength dispersion and a photomultiplier for photon detection. The actinic flux calibration of the spectroradiometer was performed before and after the campaign at the Forschungszentrum Juelich in Germany using certified irradiance standards as described in Kraus et al. (2000). Unless otherwise noted, the absorption cross-sections used to calculate photolysis frequencies were those described above; for O_3, the cross-section at 295 K was employed; for HONO the current cross-section recommendation (Sander et al., 2006) was multiplied by 1.43 in order to match recent absolute measurements of J_{HONO} (Wall et al., 2006); for CH_3CHO and CH_3COCH_3 the spectrum and quantum yield data for radical producing channels were taken from (Sander et al., 2006). Resultant J-values were multiplied by 1.08 (surface albedo) to account for the upwelling portion of the photon actinic flux. The overall uncertainties for the photolysis channels are 25% ($O_3 \rightarrow O^{1D}$, CHOCHO→radicals), 15% (HONO→OH, HCHO, CH_3CHO, CH_3COCH_3→radicals).

2.2 Radical production rate calculations

A flexible-top photochemical box model was used to calculate the radical production rates from experimentally constrained sources, and to estimate sources that were not constrained by experimental observations. The model employs the Master Chemical Mechanism (v3.1), which is based on the protocols developed by Saunders et al. (2003) and Jenkin et al. (2003), and has recently been updated for aromatic oxidation schemes (Bloss et al., 2005a, b). MCM, a near-explicit mechanism comprising 135 VOCs and more than 13.500 reactions, is ideally suited to test RO_x radical production because it contains limited chemical lumping. This enables (1) accounting of individual radical production and loss pathways; and (2) expression of RO_x radical production rates in terms of equivalent OH radical production rates (by accounting for the changing efficiency with which RO_2 and HO_2 radicals propagate into OH radicals as a function of changing experimental conditions, i.e., NO, NO_3, HO_2, RO_2 concentrations, and VOC

speciation). The box model was constrained by median time-profiles of the above radical precursor concentrations, J-values, oxidant concentrations (OH, HO_2, O_3, NO_3), and concentrations of radical sinks, i.e., 103 VOCs, NO, NO_2, SO_2, CO as detailed in Sheehy et al. (2007)[1]. The radical sinks of the constrained model matched within a few percent of experimental observations of OH-reactivity (Shirley et al., 2006). The loss mechanisms of secondary species formed via the oxidation of hydrocarbons include reaction with OH radicals, NO_3 radicals, O_3, sunlight, and dilution. The dilution term was estimated in two ways: (1) using CO as a tracer for dilution in the rising planetary boundary layer (PBL) and pollution export from the MCMA (Garcia et al., 2006), and negligible dilution during the night (this method lead to chemical accumulation of oxidation products in the code and is considered a lower limit for dilution); (2) to overcome chemical accumulation in the afternoon and at night, additional dilution was calculated to match predictions of photochemical HCHO with observations (see Sect. 3.6).

In order to estimate the nighttime radical production rates from O_3 and NO_3 radical reactions with alkenes, two scenarios were considered: (1) O_3 constrained (DOAS#1), NO_3 unconstrained; and (2) O_3 and NO_3 constrained by observations. As a first order approximation of vertical gradients in NO_3 radicals (see Sect. 3.4), the observed NO_3 by DOAS#2 was scaled linearly from differences in O_3 between DOAS#1 and DOAS#2. The scaled NO_3-concentrations were on average about a factor of 3 lower (nighttime 8 h average concentration of 1.5 pptv), and are regarded as an upper limit for the height of DOAS#1 as nonlinear feedbacks (i.e., NO_3 + NO sink reaction) are not accounted. We further base our discussion of NO_3 radicals on the (unverified) assumption that similar VOC concentrations are present in NO_3-rich and NO_3-depleted airmasses. As reactive unsaturated VOCs are expected to be depleted in O_3- and NO_3-rich air, this assumption is compatible with an upper limit estimate of the role of NO_3 radicals as a source for RO_x radicals at roof-top level. These uncertainties were minimized by constraining the box model with data collected at roof-top level (also DOAS#1 height). Finally, the sensitivity of the model towards statistical artifacts was tested by constraining with (1) average, and (2) median time-profiles of the above measurements; the results agreed within

10% at daytime, whereas larger differences were observed at night (see Sect. 3.3). Unless otherwise noted the results are reported from the median model.

2.3 Source apportionment of photochemical HCHO calculations

We used the above-mentioned box model, without the HCHO constraint, to predict the production of HCHO from hydrocarbon oxidation chemistry. The contributions from VOC classes as HCHO precursors were calculated by constraining the model for a single VOC class and the oxidants; the other VOC concentrations were set to zero. In addition, to determine the relative contribution of each oxidant, the model was run with the mechanism constrained for only that oxidant i.e., OH, O_3, NO_3, photolysis; the other oxidant concentrations were set to zero; identical sets of VOC and kinetic parameters were used. Further, to calculate the percentage of HCHO generated as first, second and higher generation VOC oxidation product, the photochemical HCHO production rate of the characteristic VOC split was characterized for mid-morning conditions: [OH] = 0.18 pptv, [O_3] = 55 ppbv and J_{NO2}=5×10^{-3} s^{-1}. The yield of photochemical HCHO is compared after 10-min and several hours of oxidation (see (Volkamer et al., 2001) for details on the argument). The small fraction of HCHO produced as a higher generation oxidation product gives some comfort that HCHO predictions from MCM are largely based on experimental constraints, rather than more uncertain structure-reactivity relationships, as they are the basis for estimates of higher generation oxidation reaction pathways.

2.4 Source apportionment of HONO calculations

MCM was constrained by measurements of relevant parameters (i.e., OH, NO, J_{HONO}, dilution) to calculate photostationary-state HONO (PSS-HONO; equilibrium concentration between the OH + NO source and photolytic sink). In some cases, PSS-HONO at night was significantly below the observations. For these cases, an additional HONO source was parameterized as a NO_2→HONO conversion rate to match the HONO pro-

duction between 08:00 p.m. to 04:00 a.m.; this "dark-HONO" source was then applied throughout the day. We employed the box model in the following two scenarios: inputs are constrained based on (1) campaign average concentration time-profiles, and (2) median concentration time-profiles. In an additional model scenario (3), only data from "cold-surge" days were averaged (de Foy et al., 2005), which are characterized by the highest relative humidity and the lowest PBL height. The highest daytime HONO concentrations are expected during such "cold-surge" events, as HONO concentrations have been shown to correlate with relative humidity (Stutz et al., 2004). In these case-studies the OH-concentration was varied within measurement uncertainty (offset of 0.01 pptv was subtracted), and J_{HONO} was multiplied by 1.43 to match recent direct measurements of J_{HONO} by Wall et al. (2006). Furthermore, both dilution cases were considered in combination with a lower limit OH-concentration and the larger value of J_{HONO}.

3 Results and discussion

3.1 OH-equivalent RO_x radical production rates

The calculated production for new RO_x from the HO_x-constrained box model is shown in Fig. 1. The total radical production rates presented in the bottom panel are shown as OH-equivalents, termed ΣOH_{new}, and account for the conversion factors in the radical propagation steps, i.e., $RO_2 \rightarrow OH$ and $HO_2 \rightarrow OH$ as is described in more detail elsewhere (Sheehy et al., 2007[1]). Figure 1 is accompanied by Table 1, which shows the percent contribution to ΣOH_{new} from various sources at selected times throughout the day, as well as day and nighttime averages. Pathways with an insignificant contribution to new RO_x formation are not shown.

The daytime ΣOH_{new} production around noon is about 25 times larger than at night. A distinct diurnal pattern is observed. Radical production rates are high already shortly after sunrise (1.8 ppb/h, or 9.6×10^6 molec/cm^3/sec at 07:00 a.m.), and then domi-

nated from production of OH radicals. It rises continuously to reach a plateau in the mid-morning (11.9 ppb/h, or 6.3×10^7 molec/cm^3/s at 10:00 a.m.). Sustained radical production persists at a high level until about 12:30 pm and begins to decrease afterwards. A continuous decrease in radical production is observed during afternoon hours until about 06:00 p.m. (1.0 ppb/h, or 5.4 x 10^6 molec/cm^3/sec at 06:00 p.m.). Radical production rates remain flat until the early morning hours. The decrease in OH, HO_2, and RO_2 radical production rates during afternoon hours coincides with decreasing O_3 concentrations, indicating that sensitive feedbacks exist between the pollution export from the MCMA and photochemical activity.

The 12-h daytime average ΣOH_{new} production (6.1 ppb/h, or 3.2×10^7 molec/cm^3/s) is dominated by OH sources, accounting on average for some 41%, while HO_2 and RO_2 account for about 40% and 19%, respectively. For the same 12-hr average, the contribution from HONO, O_3 and HCHO are roughly equal, and in sum account for more than half of all new radical production. The O_3/alkene source adds nearly 15%, with new OH- and RO_2 production contributing about equal amounts. The photolysis of secondary OVOC other than HCHO – a complex mixture of several hundred products from VOC oxidation (i.e., aldehydes, dicarbonyls, ketones, others; denoted "other OVOC" in Table 1) – account in sum for about 25% of ΣOH_{new} production. ΣOH_{new} from other OVOC is about equally formed via the formation of new HO_2 and new RO_2. Our model estimates an average daytime NO_3 radical concentration of about 0.6 pptv and about 1 pptv around noon. Daytime NO_3 radical reactions make a very small contribution to daytime equivalent OH radical sources, reflecting high NO concentrations, and the fact that radical production rates from other sources is comparably large.

During the night, the ΣOH_{new} production is determined from the reaction of alkenes with O_3 and NO_3. The 8-h nighttime average (08:00 p.m.–04:00 a.m.) ΣOH_{new} production (0.48 ppb/h, or 2.6×10^6 molec/cm^3/s) is dominated by O_3/alkene reactions. The OH and RO_2 sources contribute roughly similar amounts, and in sum account for about 80% of new equivalent-OH radical production; new HO_2 accounts for a minor radical source at night. The only direct nighttime source of OH and HO_2 radicals is the reac-

tion between O_3 and alkenes. On the other hand, for practical purposes the reactions of alkenes with NO_3 exclusively generate new RO_2 radicals. The model suggests that such NO_3/alkene reactions account for some 8–24% of nighttime new equivalent-OH production; the remaining new radical production is from O_3/alkene reactions. If we force the scaled upper limit 8-h average NO_3 radical concentration of 1.5 pptv at night (about six times the predicted values), then the reaction between NO_3 and alkenes could account on average for about half of new radical production. However, such scaled NO_3-concentrations do not account for the rapid NO_3 sink reaction with NO (see Sect. 3.3, and Fig. 3), and the actual equivalent-OH radical production rate from NO_3 at roof-top-level is likely much lower. In the near field chemical regime at roof-top-level, the NO_3/alkene source is a minor pathway for ΣOH_{new} production at night.

3.2 Production of OH, HO_2, and RO_2 radicals

Sources for OH radicals

The production of OH radicals from sources is high (3.5–4.5 ppb/h, or 1.9–2.4×10^7 molec/cm^3/s) shortly after sunrise and near constant throughout the morning. It starts to decrease after noon (12:00 p.m. CST), and is at least one order of magnitude lower at night. The predominant daytime OH radical sources are: (1) the photolysis of HONO, (2) the photolysis of O_3, and (3) the O_3/alkene reactions. In the early morning the photolysis of HONO dominates the formation of OH radicals. As photochemical O_3 accumulates, the photolysis of O_3 becomes a dominant source of OH in the late morning and throughout most of the day, accounting for about 80% at peak ozone levels. It is noteworthy that small but "non-zero" O_3-concentrations in the presence of high alkene concentrations during early hours, and unmeasured products from nighttime processing of VOCs present a significant source for OH radicals other than HONO in the early morning. Few ppb of O_3 coexist with several 10 ppb of NO shortly after sunrise, and contribute about 20% to OH production, illustrating how small changes in ozone may have a significant effect on OH radical production rates at this

time of day. Difficulties with the exact quantification of low O_3 levels exist for indirect techniques, which are widely used in current air quality monitoring networks (see discussion in Dunlea et al., 2006). An additional uncertainty exists in the speciation of alkenes, which can be affected during sample storage (Atkinson et al., 1984; Jenkin et al., 2005). OH production from O_3/alkenes is the only significant gas-phase non-photolytic source of OH during the day and at night, as NO_3-reactions do not directly form OH radicals.

Sources for HO_2 radicals

The production of HO_2 radicals is smaller than that of OH shortly after sunrise, and continuously increases to reach values around 5.4 ppb/h (or 2.9×10^7 molec/cm^3/s) around noontime. As in the case of OH, it starts to decrease after noon. New HO_2 is only a significant radical source during the day; the new HO_2 production is at least two orders of magnitude lower at night. The predominant daytime sources for HO_2 are (1) the photolysis of HCHO, and (2) the photolysis of other secondary OVOCs. HCHO photolysis accounts for more than half, the sum of other OVOCs for about 40% of the midday HO_2 production. The photolysis of CH_3CHO and O_3/alkene reactions contribute less than 2% of new HO_2 radicals throughout the day. During the night the only significant HO_2 radical source is from O_3/alkene reactions.

Sources for RO_2 radicals

The diurnal profile of RO_2 radical production is qualitatively similar to that of HO_2 radicals, though peak values around noontime are smaller (2.6 ppb/h, or 1.4×10^7 molec/cm^3/s). Also, the new RO_2 production rate is about an order of magnitude lower at night, compared to peak daytime production. The predominant daytime sources for RO_2 are the photolysis of secondary OVOCs, accounting for nearly 70% of new RO_2 radical production at midday. Some minor additional RO_2 is produced from O_3/alkene reactions and reactions of NO_3 with alkenes, phenol- and furanone-

type products of the OH-radical initiated oxidation of aromatic hydrocarbons. These reactions provide an interesting link between the RO_x and NO_x cycles; however, they only account for a minor source of RO_2 radicals (see Sect. 3.3).

Direct observations of NO_3 radicals

NO_3 radicals were detected during all nights that NO_3 measurements were attempted. The spectral proof of the successful detection is presented in Fig. 2. The highest optical density of NO_3 radical absorption was 9.6×10^{-3}, corresponding to a concentration of $(9.6\pm1.1)\times10^{8}$ molec/cm^3 or (50±6) pptv. The nighttime concentration-time profile varied between individual nights. Typically, detectable concentrations were observed during events that lasted 1–3 h. The NO_3 concentrations typically peaked around midnight (±2 h), sometimes also later in the evening, and varied between 10 and 50 pptv. The nighttime average NO_3 mixing ratio for all nights (19:00–04:00) is about 7 pptv (at DOAS#2 height). No NO_3 was detected during the afternoon hours and the early evening prior to sunset, and concentrations were below the detection limit during early morning hours. To our knowledge this is the first direct detection of NO_3 radicals in the urban core of a megacity.

The repeating pattern of periods of steeply rising NO_3 concentrations followed by periods when essentially no NO_3 is illustrated for the night from 25 April 2003 to 26 April 2003, and compared to OH radical concentrations in Fig. 3A. Also shown are the O_3 concentrations as measured by both LP-DOAS and a point-sensor, the sum of NO_2 and O_3 (O_x, from DOAS#2), and NO during that night (Fig. 3b). The good agreement in the relative variation between the point-sensor and DOAS#1 (for possible explanations for the 5–10 ppbv offset in the point sensor see Dunlea et al. (2006)) illustrates the relative homogeneity of the airmass at night. The O_x slowly decreases over the night, possibly as the result of pollution export, dry deposition, or O_x to NO_y conversion processes (such as N_2O_5 hydrolysis) inside the valley. Elevated NO_3 concentrations tend to correlate with elevated O_3, while airmasses with higher NO_2 (lower O_3) tend to contain virtually no NO_3. Nighttime OH radical concentrations are currently

not well understood and subject to ongoing debate. As shown in Fig. 3, the nighttime OH-concentration correlates better with O_3 than with NO_3 in the early evening. This is true also, though to a lesser extent, in the later night hours. However, a definitive conclusion whether O_3 or NO_3 control the nighttime OH-concentration is complicated as both gases tend to be correlated.

The simultaneous presence of O_3 and NO in a given airmass has implications for RO_2-to-OH conversion efficiencies, predicted NO_3-radical concentrations, and, to a lesser extent, OH-production rates. Figure 3c shows the comparison of the median and average concentration time profiles of O_3 (DOAS#1) and NO (point sensor). During the day there is virtually no difference between the average and median profiles, reflecting efficient mixing. At night, median concentrations are systematically lower for both O_3 and NO. The difference is larger for NO (a factor of 5–8) than for O_3 (10–80%), and reflected in the predicted NO_3-radical concentration at roof-top-level (about five times higher; median NO_3 concentrations are shown in Fig. 3c). The average lifetime of O_3 with respect to NO reactions at night is considerably longer in the median model (about 15 min; compared to about 2.5 min in the average model), i.e., long enough that the presence of both O_3 and NO in the same airmass is not mutually exclusive. Based on these results we prefer the median model for estimates of ΣOH_{new} production, which is reduced by one-third at night compared to the average model.

From the discussion presented in Sect. 3.1, it is likely that NO_3 radicals make a minor, and possibly significant contribution, to nighttime OH radical concentrations already in the near field chemical regime. The occurrence of NO_3 concentrations in episodes, and the lack of co-located open-path NO data observed in the same airmass as NO_3, makes it difficult to compare with a median model. Like NO, NO_3 radicals facilitate the cycling of RO_2 and HO_2 into OH. It is noteworthy that the propagation efficiency of RO_2 into OH radicals is controlled by NO in our model; NO_3-reactions are negligible for all cases studied. Different conditions are expected in the intermediate and far-field photochemical regime, i.e., NO_3-enriched airmasses at altitudes of several hundred meters above ground, and in the O_3-rich city plume downwind of the MCMA. In similar

airmasses, NO_3-concentrations of several hundred pptv have been observed directly (von Friedeburg et al., 2002) or inferred from N_2O_5 observations (Brown et al., 2006). Under these conditions NO is very low; the efficiency of $RO_2 \rightarrow OH$ radical conversions is controlled by NO_3-reactions, which proceed more than an order of magnitude slower than the analagous reaction involving NO; NO_3 competes with peroxi-radical self reactions which can terminate the radical chain. The efficiency for $RO_2 \rightarrow OH$ conversion is thus lower than in a high NO scenario, unless peroxi-radical self reactions propagate (vs. terminate) the radical chain. Recent evidence has been reported for such propagation to be efficient in the oxidation of acetaldehyde and acetone (Hasson et al., 2004; Jenkin et al., 2006, personal communication). If confirmed as a more general pathway, NO_3-reactions would gain relative importance as a source for OH-radicals in the intermediate- and far-field chemical regime downwind of large urban centers.

In Mexico City we did not find evidence for NO_3 radicals accumulating to measurable concentrations during the day. This is in contrast to Houston (Geyer et al., 2003), and New England (Brown et al., 2005), where daytime NO_3-concentrations have been observed, and form a non-negligible process for the oxidation of highly reactive VOC. This difference is the result of a lower NO_3-source strength (i.e., lower O_3 during afternoons) and more abundant NO_3-sink reactions in Mexico City. In contrast to Houston, biogenic VOC concentrations are much lower in Mexico City (quantified as <5% of OH-reactivity during MCMA-2003 in Volkamer et al., 2006). NO_3 reactions with anthropogenic alkenes, phenol-type and furanone-type products from aromatic hydrocarbon oxidation contribute about 26%, 36%, and 15% of the daytime RO_2 sources from NO_3-reactions, respectively, and account in sum for about 7% of the daytime NO_3-sink reactions. Daytime NO_3-reactions with furanones account for some 5–15% of the furanone lifetime in our model. The relevance of daytime NO_3-reactions, previously noted only for phenols (Kurtenbach et al., 2002), is highlighted here also for furanone-type compounds.

3.3 Characterization of horizontal and vertical gradients

Our approach uses spectroscopic measurements of trace-gas concentrations over extended spatial scales (e.g., open-path DOAS, FTIR) and highly localized "point" measurements (e.g., FIS, canisters) without further adjustments. The straightforward use of these measurements is based on the assumption that the airmass is well mixed. While this assumption almost certainly represents a simplification of the real atmosphere, it is justified here for the following reasons. Spatial gradients are expected to be strongest for primary pollutants (e.g., CO) and somewhat less pronounced for secondary pollutants (e.g., O_3). Sampled concentrations of CO and O_3 at comparable heights by point and line-averaging techniques at the CENICA supersite show excellent agreement (Dunlea et al., 2006). Further, concentrations of several species that were probed by both open-path DOAS instruments facing in different directions, spanning different spatial scales and sampling at different mean heights show excellent agreement during the day (within measurement precision). Already 1.5 h after sunrise (06:00 a.m. CST), the concentration time-traces between the two DOAS instruments have converged to within measurement precision, as is illustrated for HONO in Fig. 4. During the daytime, which is the primary focus of this study, the air mass is well mixed.

Significant differences in measurements are observed at night, when the air mass is not as well mixed. At night, mixing is driven by the heat-island effect (Jauregui, 1993; Oke et al., 1999) and large-scale eddy turbulence from mechanical sheering of winds aloft, which can lead to horizontal and vertical gradients in trace-gas concentrations. Measurements from the two DOAS instruments compared to point sampling techniques set limits on this inhomogeneity (see Figs. 3 and 4). In an attempt to minimize the effect of vertical gradients on the prediction of secondary sources, we constrain MCM with measurements of oxidants that were conducted at nearly the same height (OH, O_3). For the most precise measurements of low O_3 concentrations, we use direct measurements from DOAS#1 (for a discussion of possible interference issues with indirect techniques see Dunlea et al., 2006). Our NO_3 radical observations were

conducted at about 70 m altitude using DOAS#2, and use of these data to constrain MCM is not expected to be straightforward. While the direct detection of NO_3 radicals presents evidence of their existence at a mean height of 70 m above ground, this differs from observations at the CENICA roof-top level: An isomer-analysis of nitro-PAH samples revealed a very minor contribution of NO_3 radicals to PAH processing (Arey et al., 2004). It is noteworthy that negligible NO_3 radical concentrations are predicted at roof-top-level by MCM; this is consistent with vertical gradients possibly accounting for apparent differences. It should be noted that the O_3 measured by DOAS#1 is lower than that from DOAS#2 at higher altitude, as is shown in Fig. 3. This difference was exploited to scale NO_3-observations to account for the difference in height between DOAS#1 and DOAS#2 (see Sect. 2.2).

3.4 Source and sink considerations of HONO

The measured HONO profiles from DOAS#1 and DOAS#2 are compared with HONO predictions in Fig. 4. Regardless of the meteorological conditions, PSS-HONO accounts for at least half of the HONO concentrations at 07:00 a.m., and virtually all HONO at 09:00 a.m. Figure 4 demonstrates that a small OH-concentration in the presence of high morning NO concentrations account for ppbv-levels of HONO at 08:00 a.m. Few previous studies had simultaneous and collocated OH, NO, HONO and J_{HONO} measurements available; the interpretation of most HONO as being a radical reservoir is fully consistent with the error bars presented in Fig. 3 of Martinez et al. (2003). Additional HONO formation from dark sources, like the heterogeneous NO_2 conversion on urban surfaces (see, e.g., Arens et al., 2001; Ramazan et al., 2006, and references therein), contribute significant amounts of HONO only before 08:00 a.m. Thereafter PSS- and dark HONO sources account for essentially all of the observed HONO. Around solar noon the PSS and dark sources can account for some (35±15) pptv; these model results are robust for different meteorological conditions and independent of relative humidity. This is of the same order of magnitude as the upper limit HONO concentration that can be inferred from the DOAS#2 detection limit. Sta-

tistical averaging of DOAS#2 data yields (58±76) pptv and (21±76) pptv HONO on a campaign average and median basis; error bars correspond to one-sigma standard-deviation among individual days around solar noon. An independent quantification of daytime HONO concentrations in Mexico City remains desirable. However, it is noteworthy that photo-induced processes appear to contribute – if any – only very minor amounts to ambient HONO concentrations in Mexico City. For example, a photochemical HONO source of 5×10^{10} molec/cm^2/s from the ground (Stemmler et al., 2006), diluted in a PBL of 3 km height (typical for Mexico City), corresponds to a HONO mixing ratio of only 4.3 pptv around noon.

The characterization of daytime HONO sources in the urban atmosphere – if attempted in the future – suffers from the need to subtract a large steady-state HONO concentration. This steady-state HONO can only be quantified at the precision with which the reaction rate constant of OH with NO is known, i.e., 20% (Sander et al., 2006); in our estimate the largest uncertainty is the absolute uncertainty in OH measurements. For example, in order to quantify a photo-induced HONO concentration of 25 pptv on top of a 25 pptv PSS-HONO background with 25% uncertainty, the absolute precision of OH measurements needs to be 15% or better; such measurements are currently very difficult to achieve. High precision measurements of HONO (Kleffmann et al., 2006), NO, and J_{HONO} are necessary pre-requisites – though unlikely to be limiting – any serious efforts to quantify excess HONO over PSS-HONO in the urban atmosphere.

The following conclusions can be drawn about additional HONO sinks in urban air. We observe a significant delay in the decrease of HONO in the model if J_{HONO} is based on the value listed in Sander et al. (2006). The difference between measured and modeled HONO concentrations persist until about 10:00 a.m., as is evidenced by the inset graphs in the bottom panels of Fig. 4. This over-prediction reflects either an overestimate of HONO sources, or a missing HONO sink in the model. Since equilibrium HONO formation is a high lower limit estimate of HONO sources at that time of day, only a missing HONO sink in the model can resolve these observed differences.

Recent direct measurements of J_{HONO} reported values that were 43% higher than expected (Wall et al., 2006). By scaling J_{HONO} accordingly, we observe good agreement between the model and measurements throughout the day (see Fig. 4, lower panels). Our analysis presents independent support for the conclusion of faster-than-expected HONO photolysis (Wall et al., 2006).

3.5 Source apportionment of HCHO

Observed formaldehyde concentrations in the MCMA are a result of emissions, photochemistry, and an unknown background source, which appears to be related with a VOC chemical source (Garcia et al., 2006). Garcia et al. (2006) demonstrated that on a 24-h average basis, up to 70% of observed HCHO in the MCMA is photochemically produced. Following the procedures described in that work, we calculated the concentration time profile of HCHO from photochemical and background (chemical) sources, by subtracting an appropriately scaled tracer for HCHO emissions. Both the measured ambient HCHO, and the portion from photochemical and background sources are compared with MCM predictions in Fig. 5. The lower limit nighttime OH-concentration leads to accumulation of several ppb of HCHO (not shown), consistent with the interpretation of "background HCHO" from a chemical source (Garcia et al., 2006).

MCM was used to characterize photochemical HCHO production in terms of: (1) the relative contribution of HCHO sources by VOC class (i.e., alkanes, alkenes, aromatics, OVOCs); (2) the relative contribution of oxidants, i.e., OH, O_3, and NO_3; and (3) the portion of HCHO formed as a first vs. second (and higher) generation oxidation product. The results of the HCHO source apportionment modeling are shown in Fig. 6. On a daily average basis, we find that an overwhelming majority of the photochemical HCHO production proceeds from reactions that yield HCHO as a first generation oxidation product. The oxidation of alkenes is the major VOC precursor, and OH is the predominant oxidant that leads to the formation of photochemical HCHO in the MCMA. The O_3/alkene source, while significant, only accounts for some 17% of the photochemical HCHO production. The aromatic species make a smaller contribution,

and are largely responsible for secondary HCHO production. NO_3 radical initiated oxidation of VOCs and photolysis reactions are insignificant compared to other sources of HCHO in the MCMA.

3.6 Comparison of Mexico City with other case studies

In the following the radical production rate in the MCMA is compared to that in Nashville (Martinez et al., 2003), Pabsthum downwind of Berlin (Alicke et al., 2003), New York City (NYC) (Ren et al., 2003), Milan (Alicke et al., 2002), Birmingham (Emmerson et al., 2005), Chelmsford downwind of London (Emmerson et al., 2007), rural environments (Zhou et al., 2002; Kleffmann et al., 2005; Acker et al., 2006) and the free troposphere (Singh et al., 1995; Arnold et al., 2004).

3.7 Timing of radical production

It is generally expected that the radical production rate during summer follows the abundance of sunlight and peaks around the time of lowest solar zenith angle (solar noon). Such correlations are indeed observed in NYC, Nashville, rural environments and also during cleaner days in Pabsthum and Milan. There is only limited information given about the timing of radical production in Birmingham and Chelmsford, though the choice of averaging times in the presentation of the results from those studies (11:00 a.m.–03:00 p.m., centred around solar noon), and the relative importance of photolytic sources may be indicative of such correlation during summertime. Alternatively, a radical pulse from HONO in the early morning, decreasing radical production rate in the mid-morning (i.e., a dip), followed by a local maximum radical production rate around solar noon has been observed during individual days in Milan and Pabsthum.

In Mexico City, we did not observe a symmetric radical production rate around solar noon, nor did we observe a dip in the mid-morning. Rather, the peak of new radical production is systematically shifted towards mid-morning, i.e., around 10:00 a.m. or three hours before solar noon (see Fig. 1). It is sustained at this high level until pollu-

tion is efficiently exported from the MCMA. The absence of both a morning peak and a mid-morning dip in the radical production rate is attributed to the particularly high rate from secondary sources (all formed as a result of photochemical processing of pollutants): photolysis of HCHO, O_3, and other OVOCs in sum contribute about 75% of the radical production rate around 11:00 a.m., and 85% around 01:00 p.m. In other words, whatever radical source starts the processing of pollutants gets amplified by further radical production from secondary pollutants; the surrounding mountains trap secondary pollutants within the basin during mid-morning. Our analysis highlights two phenomena: (1) the importance of radical sources that start the photochemical processing in the early morning, and (2) the non-linear feedbacks between meteorology (i.e., pollution export) and photochemical activity in the MCMA. These feedbacks have not been previously quantified at the radical level (i.e., radical production rates).

Absolute radical source strength

The overall radical production rate in the MCMA is higher than has been observed in any previous study. The radical production rate averaged over a 4-h time window centred near its peak is about 1.7 times higher than in Milan, 2 times that observed in Birmingham during summertime, 2.7 times that in Chelmsford, and 3 times higher than in Birmingham during wintertime. It is 3.3 times higher than in New York City and Nashville, 3.5 times higher than in Pabsthum, and 7–10 times that in rural environments. This comparison highlights the unique chemical activity of the Mexico City atmosphere.

Furthermore, the 24-h average HO_x radical production rate in the upper troposphere – 2.3×10^4 molec/cm^3/s (Singh et al., 1995; Arnold et al., 2004) – is two to three orders of magnitude lower than in the MCMA. Recently, higher than expected concentrations of oxygenated hydrocarbons have been measured in the free troposphere (Kwan et al., 2006). Interestingly, new HO_x production rates from CH_3CHO and CH_3COCH_3 in Mexico City are comparable to those in the free troposphere, about 5 x10^5 and

10^4 molec/cm^3/s respectively (11 km height, solar zenith angle SZA = 15 degrees, [CH_3CHO] = 200 pptv, [CH_3COCH_3] = 500 pptv). While O_3 or HCHO photolysis are important radical sources in both of these very different compartments of the atmosphere, the higher-than-expected concentrations of CH_3CHO in the free troposphere coupled with faster photolysis at higher altitude lead to HO_x production rates that compare or or even exceed that from O_3 and HCHO photolysis, emphasizing the role of radical sources other than ozone at high altitude (Frost et al., 1999). The relevance of the polluted urban atmosphere as a source for oxidized hydrocarbons is expected to increase in the future.

Relative importance of different radical sources

The average daytime contribution to radical production rates from different sources in the MCMA is compared to other urban influenced environments in Table 2. Remarkably, the distribution of radical sources in the MCMA is fairly even; there is not a single radical source that dominates (with variation of less than a factor of two amongst those listed; for time-of-day dependent discussion see Table 1, and Sects. 3.1 and 3.8). This is different from previously studied atmospheres, in which typically one radical source dominates: HONO in NYC; HCHO in Milan; O_3 in Nashville, O_3/alkene reactions in Birmingham during wintertime, secondary OVOC in Birmingham and Chelmsford during summertime. Downwind of Berlin, in Pabsthum, O_3 and HCHO photolysis are both particularly important. Despite the considerable variability among different urban polluted, and between urban and rural atmospheres, some generalizations can be drawn.

HONO photolysis: We have included HONO among the radical sources in Tables 1 and 2, neglecting the fact that throughout most of the day a significant portion of HONO appears to be a radical reservoir instead of a radical source in the MCMA. At 09:00 a.m. virtually all HONO is accounted as PSS-HONO; if HONO was accounted based on the net-flux the contribution from other sources would be higher. Rather than reflecting net-production (i.e., sources minus sinks of OH radicals) the numbers in our tables reflect

absolute radical production rate from HONO, as we feel that any other representation would bias low the relevance of HONO during morning hours. HONO photolysis makes an important contribution to jump-starting photochemistry in the early morning (Platt et al., 1980), though it is not the only radical source at that time of day in the MCMA.

Recently, significant daytime HONO concentrations in rural and forested environments indicate the presence of additional daytime HONO sources that are up to 64 times greater than the nighttime sources, and comparable to other sources like HCHO and O_3-photolysis (Zhou et al., 2002; Kleffmann et al., 2005; Acker et al., 2006). The only laboratory study that could thus far present convincing evidence for atmospheric relevance is that by Stemmler et al. (2006). This photo-induced HONO source strength contributes about 0.3% to the ΣOH_{new} sources in the MCMA. Even a ten-fold increase in surface area (which in Mexico City is mostly due to abundant aerosol surface area, and only to a lesser extent due to vertical building surfaces) would make an insignificant contribution (~3%) to the overall noontime radical production rate here. Our observations are incompatible with findings in NYC, where HONO measurements with a wet-chemical technique (scrubbed derivatization HPLC) suggest high noontime radical production rates (about 10^7 molec/cm^3/s, or ten times the likely estimate, and twice the upper limit set by our measurements) corresponding to about 300 pptv of HONO. These high daytime HONO concentrations are directly observable with currently available spectroscopic techniques. Strong apparent differences in the relative importance of HONO as a radical source seem to exist in different polluted urban environments. Between NYC and the MCMA, differences exist in the types of available surface areas, the availability of sunlight in street-canyons, the vertical mixing-height and horizontal dispersion of pollutants. A direct confirmation of the HONO levels in NYC remains desirable.

HCHO-photolysis: The contribution from this source is highly variable. Compared to other urban environments, it is lower in the MCMA than downwind of Milan, Berlin and Nashville, but higher than in NYC, Birmingham and downwind of London. HCHO is an important radical source in the MCMA. About 70% of the average daytime radical

production rate from HCHO is attributed to HCHO that forms from secondary sources (hydrocarbon photochemistry) (Garcia et al., 2006).

HCHO is emitted in significant amounts as part of vehicle exhaust in the MCMA (Zavala et al., 2006; Garcia et al., 2006). Conversely, targeted reductions of primary HCHO sources present an opportunity to slow down the rate of hydrocarbon oxidation. While primary HCHO only accounts for about 30% of the average daytime radical production rate from HCHO-photolysis, the contribution peaks at around 09:00 a.m., when the net-radical production rate from other sources is either no longer (HONO), or not yet (O_3) efficient. Primary HCHO sources contribute about 10% of the overall net-production of radicals before 10 am, and contribute significantly to the formation of those secondary species which sustain the exceptionally high ΣOH_{new} production in the mid-morning. Reductions in primary HCHO sources can thus be expected to yield additional benefits from reducing the production rate of secondary species. Such amplification of benefits may however be out-weighed by parameters such as cycling chain length (Sheehy et al., 2007[1]), which is highest in the early morning hours and decreasing towards the mid-morning, when primary HCHO contributes most to ΣOH_{new}. From a radical source perspective, the potential benefits of targeted primary HCHO reductions to reduce peak concentrations of secondary species like O_3 and SOA warrant future investigation. A necessary prerequisite for future modeling attempts on this subject will be to develop models that adequately represent radical sources other than HCHO.

O_3-photolysis: The contribution from this source exceeds 30% only in semi-polluted and rural environments; it is generally below or close to 20% in more polluted environments, like Milan, NYC, and – interestingly – the MCMA. Despite frequent O_3 exceedances of 100 ppbv in the MCMA, its location at 2220 m above sea level and tropical latitude, the daily average contribution from O_3 photolysis is not higher than that observed in other polluted atmospheres. This reflects efficient venting of the MCMA during afternoons, and the abundance of other radical sources. The moderate contribution from O_3 photolysis in the urban atmosphere also means that any correlation of

OH radical concentrations with J_{O3} is rather a reflection of the fact that 85% of radical production is light-induced. Any such correlation should not be mistaken as evidence that O_3 indeed controls OH radical concentrations in the urban atmosphere.

O_3/alkene reactions: A markedly different contribution from O_3/alkene sources is observed compared to previous studies. Notably, in the MCMA, the radical contribution from O_3/alkene reactions is about five times higher compared to the alkene abundance, i.e., 3–6% ppbC at CENICA (Velasco et al., 2007). In estimating the role of alkene reactions, it is necessary to consider the oxidation of alkenes by OH as the predominant source for photochemical HCHO in Mexico City (see Sect. 3.6); photochemical sources are also the predominant source of ambient HCHO during the day (Garcia et al., 2006). In addition, O_3/alkene reactions are the predominant source for OH radicals at night, leading to the accumulation of secondary pollutants that produce radicals in the early morning hours. Further, the storage of nighttime OH-radicals in the form of PSS-HONO makes an important contribution to morning HONO levels. Photolysis of PSS-HONO, other OVOC and O_3/alkene reactions in sum are responsible for about 75% of the radical production rate one hour after sunrise. Notably, the three studies that employed a detailed chemical mechanism to study radical sources (Emmerson et al., 2005, 2007; this work) yield the highest estimates for the contribution from O_3/alkene reactions; lumped chemical codes seem to give lower estimates of O_3/alkene sources (see Table 2). O_3/alkene reactions make an important radical source during winter in Birmingham (Emmerson et al., 2005). The combined radical production rate attributable to alkene reactions exceed that from any other source in the early morning in Mexico City.

Photolysis of secondary OVOC (other than HCHO): Most studies do not account for the radical production from the photolysis of OVOC other than HCHO, which contribute some 27% to the 12-h average daytime radical production rate during MCMA-2003. Again, the two other studies available for comparison at this level of detail (Emmerson et al., 2005, 2007) indicate a comparable contribution in the winter, and two times higher contribution during summer. We did not find any information whether active measures were taken in Emmerson et al. (2005, 2007) to avoid the chemical

accumulation of OVOC that we observed in our model: if pollution export from the MCMA is neglected (see Sect. 2.2), about twice as high contribution from OVOC was observed. Pollution export from the MCMA has important feedbacks to lower radical production rate inside the basin.

3.8 Implications for Mexico City air quality

The peak concentrations of secondary pollutants, like O_3 have decreased in recent years in Mexico City (Molina and Molina, 2002). It is presently not clear whether this is the result of (1) reductions in hydrocarbon emissions (VOC sensitivity of O_3 production), (2) a delay in the formation of O_3 (NO_x suppressed O_3 formation in the early morning), or (3) reductions in light intensity near ground as a result of increasing light-absorbing PM pollution; any combination is indeed possible. In any of these scenarios the formation of secondary pollutants is radical-limited. Figure 7 shows radical sources grouped into primary (emission related) and secondary (photochemistry related) radical sources. In light of the amplification of early morning sources by secondary pollutants, reactions of anthropogenic alkenes are found to be particularly important; a lower limit for the radical production rate related to alkenes (either directly or indirectly) is also included in Fig. 7. Reductions in VOC emissions (in particular alkenes) would induce further reductions in peak concentrations of secondary pollutants like O_3 or SOA in three ways: (1) by lowering the rate of VOC oxidation as a result of a lower VOC/NO_x ratio (effect of a lower radical re-cycling efficiency), (2) by slowing down the formation of secondary pollutants (effect of a lower radical production rate during the day and at night), and (3) by delaying the onset of photochemical processing; peak concentrations of secondary pollutants are capped by pollution export from the MCMA (effect of reducing the time available to produce secondary pollutants), see Sect. 3.1. To our knowledge, only pathway (1) has previously been associated with VOC reductions, pathways (2) and (3) reflect additional feedbacks that are demonstrated in this study.

ACPD
7, 5365–5412, 2007

EGU

4 Conclusions and outlook

A detailed chemical code has been constrained by an extensive set of chemical and meteorological measurements to analyze radical sources in the Mexico City Metropolitan Area. During the day, more than 70% of RO_x radical sources are constrained by observations; this portion is higher during the night. Photo-induced HONO sources contribute <3% to the radical production rate around noontime; furthermore HONO photolysis is found to be faster than expected. The photolysis of secondary OVOC other than HCHO contributes little to the overall radical production. The sum of several hundred compounds contributes about 27% on a 12-h daytime average basis, reflecting that (1) photolysis quantum yields of most carbonyls are significantly below unity, and (2) efficient pollution export in the afternoon has important feedbacks to lower radical production from secondary OVOC.

Radical production does not follow the abundance of sunlight. Rather, the peak radical production is systematically shifted towards mid-morning, around 10:00 a.m. or three hours before solar noon. It is sustained at high levels until pollution is efficiently exported from the MCMA. The formation of secondary pollutants is identified as being particularly sensitive to alkene reactions, which are directly or indirectly responsible for 75% of the radical production rate in the early morning, about an hour after sunrise. Early morning radical production becomes amplified in the mid-morning from secondary sources (i.e., HCHO, O_3 and secondary OVOC photolysis), reflecting how the trapping of pollutants within the MCMA basin leads to particularly high radical production rate and active photochemistry. The particularly high contribution of alkene related morning radical sources in the MCMA reduces the solar zenith angle dependence of "photo"chemical smog formation in the MCMA, where high radical production rates are expected year-round.

Anthropogenic alkenes are deemed to add little organic mass to secondary organic aerosol (SOA) formation in urban atmospheres: known alkene-type SOA precursors contribute <2% of SOA mass in Mexico City (Volkamer et al., 2006); considerable

ACPD
7, 5365–5412, 2007

uncertainty exists about SOA sources in the polluted atmosphere (Volkamer et al., 2006; Robinson et al., 2007). While alkenes appear to add little SOA mass directly, they indirectly add to SOA by providing radicals for the processing of other SOA precursor VOCs. While the chemical identity of most SOA precursors remains to be discovered, O_3/alkene reactions largely control the rate of hydrocarbon oxidation by a time when a significant missing SOA source is operative in the MCMA (Volkamer et al., 2006). This indirect SOA contribution of alkenes, i.e. to control oxidant fields, is likely to be much larger than their direct contribution to SOA formation. Three pathways are identified by which reductions in VOC emissions (in particular alkenes) benefit reductions in peak concentrations of secondary pollutants like O_3 or SOA (see Sect. 3.8).

NO_3/VOC reactions are found to contribute little to radical production at roof-top-level, but contribute to the removal of furanone-type and phenol-type compounds during the day, and are expected to gain relative importance in the photochemical plume downwind of the MCMA. We present to our knowledge the first direct observation of NO_3 radicals in the urban center of a megacity.

Future studies of radical sources in the polluted atmosphere need to take active measures to control the possibility of sampling artifacts with (1) the quantification of low O_3 levels (Dunlea et al., 2006) which may bias any results related to alkenes, accomplished here by using spectroscopic techniques for the direct detection of O_3; (2) alkene quantification and speciation by off-line analytical techniques (Atkinson et al., 1984; Jenkin et al., 2005), minimized here to the best possible degree by using a combination of an on-line FIS sensor, supplemented by VOC canister samples (Velasco et al., 2007). A direct confirmation of the alkene speciation by on-line techniques remains desirable in the MCMA. Finally, the degree to which models could possibly capture the amplification of benefits from VOC reductions (see Sect. 3.8) may depend on the level of detail represented in the respective underlying chemical codes. It remains to be verified whether important details such as radical production from O_3/alkene reactions are adequately represented in simplified chemical schemes.

Finally, there exists bias in the current literature, as most observations are made

in airmasses near the ground; little is known about how representative those observations are for the planetary boundary layer. Extrapolation from surface observations may not be straightforward due to the possibility of vertical gradients; satellite data in turn provide only limited information about the vertical distribution of trace-gases. Future efforts need to assess the vertical distribution of relevant radical precursors in the MCMA and throughout the troposphere. In the MCMA efforts are underway as part of the MILAGRO and MCMA-2006 field campaigns.

Acknowledgements. We are grateful to U. Platt for lending us the DOAS and spectroradiometer equipment, and to T. Jobson, L. Alexander and P. Prazeller for providing unpublished acetone and acetaldehyde measurements. We thank C. Hak, J. Bossmeyer and K. Johnson for their help in setting up the instrument, staff at CENICA and at Museo Fuego Nuevo for their hospitality during the campaign, and colleagues at Forschungszentrum Juelich for helping with the spectroradiometer calibration. M. Trainer and S. Brown provided helpful comments on the manuscript. Financial support from National Science Foundation (ATM-0528227), Department of Energy (DE-FG02-0563980), Alliance for Global Sustainability (AGS), and Comisión Ambiental Metropolitana (CAM) is gratefully acknowledged. R. Volkamer acknowledges consecutive fellowships by the Henry & Camille Dreyfus Foundation and Alexander von Humboldt Foundation.

References

Acker, K., Moller, D., Wieprecht, W., Meixner, F. X., Bohn, B., Gilge, S., Plass-Dulmer, C., and Berresheim, H.: Strong daytime production of OH from HNO2 at a rural mountain site, Geophys. Res. Lett., 33, L02809, doi:10.1029/2005GL024643, 2006.

Alicke, B., Geyer, A., Hofzumahaus, A., Holland, F., Konrad, S., Patz, H. W., Schafer, J., Stutz, J., Volz-Thomas, A., and Platt, U.: OH formation by HONO photolysis during the BERLIOZ experiment, J. Geophys. Res.-Atmos., 108, 8247–8263, doi:10.1029/2001JD000579, 2003.

Alicke, B., Platt, U., and Stutz, J.: Impact of nitrous acid photolysis on the total hydroxyl radical budget during the Limitation of Oxidant Production/Pianura Padana Produzione di Ozono study in Milan, J. Geophys. Res.-Atmos., 107, 8196, doi:10.1029/2000JD000075, 2002.

Arens, F., Gutzwiller, L., Baltensperger, U., Gaggeler, H. W., and Ammann, M.: Heterogeneous reaction of NO2 on diesel soot particles, Environ. Sci. Technol., 35, 2191–2199, doi:10.1021/es000207s, 2001.

Arey, J., Bethel, H. L., Reisen, F., and Brune, W. H.: Nitro-PAHs in Mexico City: Can Their Presence Be Attributed to Hydroxyl Radical Reactions?, Eos Trans. AGU, 85(47), Fall Meet. Suppl., Abstract A14A-02, 2004.

Arnold, S. R., Chipperfield, M. P., Blitz, M. A., Heard, D. E., and Pilling, M. J.: Photodissociation of acetone: Atmospheric implications of temperature-dependent quantum yields, Geophys. Res. Lett., 31, L07110, doi:10.1029/2003GL019099, 2004.

Arriaga-Colina, J. L., West, J.J., Sosa, G., Escalona, S. S., Ordunez, R. M., and Cervantes, A. D. M.: Measurements of VOCs in Mexico City (1992-2001) and evaluation of VOCs and CO in the emissions inventory, Atmos. Environ., 38, 2523–2533, doi:10.1016/j.atmostenv.2004.01.033, 2004.

Atkinson, R., Aschmann, S. M., Winer, A. M., and Pitts, J. N.: Gas-Phase Reaction of No2 with Alkenes and Dialkenes, Intl. J. Chem. Kin., 16, 697–706, doi:10.1002/kin.550160607, 1984.

Bass, A. M. and Paur, R. J.: UV Absorption Cross-Sections for Ozone - the Temperature-Dependence, J. Photochem., 17, 141, doi:10.1016/0047-2670, 1981.

Bell, M. L., McDermott, A., Zeger, S. L., Samet, J. M., and Dominici, F.: Ozone and short-term mortality in 95 US urban communities, 1987-2000, J. Am. Med. Assoc., 292, 2372–2378, 2004.

Bloss, C., Wagner, V., Bonzanini, A., Jenkin, M. E., Wirtz, K., Martin-Reviejo, M., and Pilling, M. J.: Evaluation of detailed aromatic mechanisms (MCMv3 and MCMv3.1) against environmental chamber data, Atmos. Chem. Phys., 5, 623–639, 2005a.

Bloss, C., Wagner, V., Jenkin, M. E., Volkamer, R., Bloss, W. J., Lee, J. D., Heard, D. E., Wirtz, K., Martin-Reviejo, M., Rea, G., Wenger, J. C., and Pilling, M. J.: Development of a detailed chemical mechanism (MCMv3.1) for the atmospheric oxidation of aromatic hydrocarbons, Atmos. Chem. Phys., 5, 641–664, 2005b.

Brown, S. S., Osthoff, H. D., Stark, H., Dube, W. P., Ryerson, T. B., Warneke, C., de Gouw, J. A., Wollny, A. G., Parrish, D. D., Fehsenfeld, F. C., and Ravishankara, A. R.: Aircraft observations of daytime NO3 and N2O5 and their implications for tropospheric chemistry, J. Photochem. Photobio. A-Chem., 176, 270–278, doi:10.1016/j.jphotochem.2005.10.004, 2005.

Brown, S. S., Ryerson, T. B., Wollny, A. G., Brock, C. A., Peltier, R., Sullivan, A. P., Weber, R. J., Dube, W. P., Trainer, M., Meagher, J. F., Fehsenfeld, F. C., and Ravishankara, A. R.:

Variability in nocturnal nitrogen oxide processing and its role in regional air quality, Sci., 311, 67–70, doi:10.1126/science.1120120, 2006.
Cantrell, C. A., Davidson, J. A., McDaniel, A. H., Shetter, R. E., and Calvert, J. G.: Temperature-Dependent Formaldehyde Cross-Sections in the Near-Ultraviolet Spectral Region, J. Phys. Chem., 94, 3902–3908, doi:10.1021/j100373a008, 1990.
Carter, W.P.L., Environmental Chamber Studies of Ozone Formation Potentials of Volatile Organic Compounds. Rudzinski, K. and Barnes, I. (Eds.), Proceedings of the NATO Advanced Research Workshop "Environmental Simulation Chambers: Application to Atmospheric Chemical Processes", Zakopane, Poland 1- 4 October, 2004, NATO Sciences Series, IV. Earth and Environmental Sciences. Vol. 62. Kluwer Publishing, Doortrecht, The Netherlands, 2005.
Davis, D. L., Bell, M. L., and Fletcher, T.: A look back at the London smog of 1952 and the half century since, Environ. Health Perspec., 110, A734–A735, 2002.
Dunlea, E. J., Herndon, S. C., Nelson, D. D., Volkamer, R., Lamb, B. K., Allwine, E. J., Grutter, M., Ramos Villegas, C. R., Marquez, C., Blanco, S., Cardenas, B., Kolb, C. E., Molina, L. T., and Molina, M. J.: Technical note: Evaluation of standard ultraviolet absorption ozone monitors in a polluted urban environment, Atmos. Chem. Phys., 6, 3136–3180, 2006, http://www.atmos-chem-phys.net/6/3136/2006/.
Emmerson, K. M., Carslaw, N., and Pilling, M. J.: Urban atmospheric chemistry during the PUMA campaign 2: Radical budgets for OH, HO2 and RO2, J. Atmos. Chem., 52, 165–183, doi:10.1007/s10874-005-1323-2, 2005.
Emmerson, K. M., Carslaw, N., Carslaw, D. C., Lee, J. D., McFiggans, G., Bloss, W. J., Gravestock, T., Heard, D. E., Hopkins, J., Ingham, T., Pilling, M. J., Smith, S. C., Jacob, M., and Monks, P. S.: Free radical modelling studies during the UK TORCH Campaign in Summer 2003, Atmos. Chem. Phys., 7, 167–181, 2007, http://www.atmos-chem-phys.net/7/167/2007/.
Fayt, C. and van Roozendael, M.: WinDoas 2.1 – Software User Manual. 2001. Brussels: BIRA-IASB.
Fuhrer, J. and Booker, F.: Ecological issues related to ozone: agricultural issues, Environ. Intl., 29, 141–154, doi:10.1016/S0160-4120(02)00157-5, 2003.
Frost, G. J., Trainer, M., Mauldin, R. L., Eisele, F. L., Prevot, A. S. H., Flocke, S. J., Madronich, S., Kok, G., Schillawski, R. D., Baumgardner, D., and Bradshaw, J.: Photochemical modeling of OH levels during the first aerosol characterization experiment (ACE 1), J. Geophys. Res.-

Atmos., 104, 16 041–16 052, doi:10.1029/1999JD900196, 1999.
Garcia, A. R., Volkamer, R., Molina, L. T., Molina, M. J., Samuelsson, J., Mellqvist, J., Galle, B., Herndon, S., and Kolb, C. E.: Separation of emitted and photochemical formaldehyde in Mexico City using a statistical analysis and a new pair of gas-phase tracers, Atmos. Chem. Phys., 5, 4545–4557, 2006, http://www.atmos-chem-phys.net/5/4545/2006/.
Geyer, A., Alicke, B., Ackermann, R., Martinez, M., Harder, H., Brune, W., di Carlo, P., Williams, E., Jobson, T., Hall, S., Shetter, R., and Stutz, J.: Direct observations of daytime NO3: Implications for urban boundary layer chemistry, J. Geophys. Res.-Atmos., 108, 4368, doi:10.1029/2002JD002967, 2003.
Gomer, T., Brauers, T., Heintz, F., Stutz, J., and Platt, U.: MFC User Manual, Version 1.98, Institut fuer Umweltphysik, University of Heidelberg., 1993.
Gregg, J. W., Jones, C. G., and Dawson, T. E.: Urbanization effects on tree growth in the vicinity of New York City, Nat., 424, 183–187, doi:10.1038/nature01728, 2003.
Haagen-Smit, A. J., Darley, E. F., Zaitlin, M., Hull, H., and Noble, W.: Investigation on injury to plants from air pollution in the Los Angeles area, Plant Physio., 27, 18, 1951.
Hasson, A. S., Tyndall, G. S., and Orlando, J. J.: A product yield study of the reaction of HO2 radicals with ethyl peroxy (C2H5O2), acetyl peroxy(CH3C(O)O-2), and acetonyl peroxy (CH3C(O)CH2O2) radicals, J. Phys. Chem. A, 108, 5979–5989, doi:10.1021/jp048873t, 2004.
Health Effects Institute. Reanalysis of the Harvard Six Cities Study and the American Cancer Society Study of Particulate Air Pollution and Mortality: A Special Report of the Institute's Particle Epidemiology Reanalysis Project. Library of Congress Catalog Number for the HEI Report Series: WA 754 R432. Health Effects Instit., Cambridge, MA, 2000.
IPCC. A Report of Working Group I of the Intergovernmental Panel on Climate Change: Summary for Policymakers, http://www.ipcc.ch/, 2007.
Jauregui, E.: Mexico City's urban heat island revisited, Erdkunde, 47, 185–195, 1993.
Jenkin, M. E., Andersen, M. P. S., Hurley, M. D., Wallington, T. J., Taketani, F., and Matsumi, Y.: A kinetics and mechanistic study of the OH and NO2 initiated oxidation of cyclohexa-1,3-diene in the gas phase, Phys. Chem. Chem. Phys., 7, 1194–1204, doi:10.1039/b417525e, 2005.
Jenkin, M. E., Saunders, S. M., Wagner, V., and Pilling, M. J.: Protocol for the development of the Master Chemical Mechanism, MCM v3 (Part B): tropospheric degradation of aromatic

volatile organic compounds, Atmos. Chem. Phys., 3, 181–193, 2003, http://www.atmos-chem-phys.net/3/181/2003/.
Kleffmann, J., Gavriloaiei, T., Hofzumahaus, A., Holland, F., Koppmann, R., Rupp, L., Schlosser, E., Siese, M., and Wahner, A.: Daytime formation of nitrous acid: A major source of OH radicals in a forest, Geophys. Res. Lett., 32, L05818, doi:10.1029/2005GL022524, 2005.
Kleffmann, J., Lorzer, J. C., Wiesen, P., Kern, C., Trick, S., Volkamer, R., Rodenas, M., and Wirtz, K.: Intercomparison of the DOAS and LOPAP techniques for the detection of nitrous acid (HONO), Atmos. Environ., 40, 3640–3652, doi:10.1016/j.atmosenv.2006.03.027, 2006.
Kraus, A., Rohrer, F., and Hofzumahaus, A.: Intercomparison of NO2 photolysis frequency measurements by actinic flux spectroradiometry and chemical actinometry during JCOM97, Geophys. Res. Lett., 27, 1115–1118, 2000.
Kurtenbach, R., Ackermann, R., Becker, K. H., Geyer, A., Gomes, J. A. G., Lorzer, J. C., Platt, U., and Wiesen, P.: Verification of the contribution of vehicular traffic to the total NMVOC emissions in Germany and the importance of the NO3 chemistry in the city air, J. Atmos. Chem., 42, 395–411, doi:10.1023/A:1015778616796, 2002.
Kwan, A. J., Crounse, J. D., Clarke, A. D., Shinozuka, Y., Anderson, B. E., Crawford, J. H., Avery, M. A., McNaughton, C. S., Brune, W. H., Singh, H. B., and Wennberg, P. O.: On the flux of oxygenated volatile organic compounds from organic aerosol oxidation, Geophys. Res. Lett., 33, L15815, doi:10.1029/2006GL026144, 2006.
Lei, W., de Foy, B., Zavala, M. A., Volkamer, R., and Molina, L. T.: Characterizing ozone production in the Mexico City Metropolitan Area: a case study using a chemical transport model, Atmos. Chem. Phys., 7, 1347–1366, 2007, http://www.atmos-chem-phys.net/7/1347/2007/.
Martinez, M., Harder, H., Kovacs, T. A., Simpas, J. B., Bassis, J., Lesher, R., Brune, W. H., Frost, J. G., Williams, E. J., Stroud, C. A., Jobson, B. T., Roberts, J. M., Hall, S. R., Shetter, R. E., Wert, B., Fried, A., Alicke, B., Stutz, J., Young, V. L., White, A. B., and Zamora, R. J.: OH and HO2 concentrations, sources, and loss rates during the Southern Oxidants Study in Nashville, Tennessee, summer 1999, J. Geophys. Res.-Atmos., 108, 4617–4633, doi:10.1029/2003JD003551, 2003.
Molina, M. J. and Molina, L. T., Air Quality in the Mexico Megacity: An Integrated Assessment, pp. 105–136, Kluwer Academic Publishers, Dordrecht,The Netherlands, 2002.
Nel, A.: Air Pollution–Related Illness: Effects of Particles, Sci., 308, 804–806,

doi:10.1126/science.1108752, 2005.
Oke, T. R., Spronken-Smith, R. A., Jauregui, E., and Grimmond, C. S. B.: The energy balance of central Mexico City during the dry season, Atmos. Environ., 33, 3919–3930, doi:10.1016/S1352-2310(99)00134-X, 1999.
Orphal, J.: A critical review of the absorption cross-sections of O-3 and NO2 in the ultraviolet and visible, J. Photochem. Photobio. A-Chem., 157, 185–209, doi:10.1016/S1010-6030(03)00061-3, 2003.
PAPA, Public Health and Air Pollution in Asia (PAPA) Special Report 15: Health Effects of Outdoor Air Pollution in Developing Countries of Asia. Library of Congress Catalog Number for the HEI Report Series: WA 754 R432. Health Effects Institute, Cambridge, MA, 2004.
Platt, U.: Differential Optical Absorption Spectroscopy, in Monitoring by Spectroscopic Techniques, edited by M. W. Sigrist, 27–84, Wiley & Sons, New York, 1994.
Platt, U., Perner, D., Harris, G. W., Winer, A. M., and Pitts, J. N.: Observations of Nitrous-Acid in An Urban Atmosphere by Differential Optical-Absorption, Nat., 285, 312–314, doi:10.1038/285312a0, 1980.
Pope, C. A., Burnett, R. T., Thun, M. J., Calle, E. E., Krewski, D., Ito, K., and Thurston, G. D.: Lung cancer, cardiopulmonary mortality, and long-term exposure to fine particulate air pollution, J. Amer. Med. Assoc., 287, 1132–1141, 2002.
Ramanathan, V., Crutzen, P. J., Kiehl, J. T., and Rosenfeld, D.: Atmosphere - Aerosols, Climate, and the Hydrological Cycle, Sci., 294, 2119–2124, doi:10.1126/science.1064034, 2001.
Ramazan, K. A., Wingen, L. M., Miller, Y., Chaban, G. M., Gerber, R. B., Xantheas, S. S., and Finlayson-Pitts, B. J.: New experimental and theoretical approach to the heterogeneous hydrolysis of NO2: Key role of molecular nitric acid and its complexes, J. Phys. Chem. A, 110, 6886–6897, doi:10.1021/jp056426n, 2006.
Ren, X. R., Harder, H., Martinez, M., Lesher, R. L., Oliger, A., Simpas, J. B., Brune, W. H., Schwab, J. J., Demerjian, K. L., He, Y., Zhou, X. L., and Gao, H. G.: OH and HO2 Chemistry in the urban atmosphere of New York City, Atmos. Environ., 37, 3639–3651, doi:10.1016/S1352-2310(03)00459-X, 2003.
Robinson, A. L., Donahue, N. M., Shrivastava, M. K., Weitkamp, E. A., Sage, A. M., Grieshop, A. P., Lane, T. E., Pierce, J. R., and Pandis, S. N.: Rethinking organic aerosols: Semivolatile emissions and photochemical aging, Sci., 315, 1259–1262, doi:10.1126/science.1133061, 2007.
RuizSuarez, L. G., Castro, T., Mar, B., Ruizsantoyo, M. E., and Cruz, X.: Do We Need An

Ad Hoc Chemical Mechanism for Mexico-City Photochemical Smog, Atmos. Environ. Part A-General Topics, 27, 405–425, 1993.

Salcedo, D., Onasch, T. B., Dzepina, K., Canagaratna, M. R., Zhang, Q., Huffman, J. A., de-Carlo, P. F., Jayne, J. T., Mortimer, P., Worsnop, D. R., Kolb, C. E., Johnson, K. S., Zuberi, B., Marr, L. C., Volkamer, R., Molina, L. T., Molina, M. J., Cardenas, B., Bernabe, R. M., Marquez, C., Gaffney, J. S., Marley, N. A., Laskin, A., Sutthanandan, V., Xie, Y., Brune, W.H., Lesher, R., Shirley, T. R., and Jimenez, J. L.: Characterization of Ambient Aerosols in Mexico City during the MCMA-2003 Campaign with Aerosol Mass Spectrometry: Results at the CENICA Supersite, Atmos. Chem. Phys., 6, 925–946, 2006, http://www.atmos-chem-phys.net/6/925/2006/.

Sander, S. P., Friedl, R. R., Golden, D. M., Kurylo, M. J., Moortgat, G. K., Keller-Rudeck, H., Wine, P. H., Ravishankara, A. R., Kolb, C. E., Molina, M. J., Finlaysson-Pitts, B. J., Huie, R. E., and Orkin, R. L.: Chemical Kinetics and Photochemical Data for Use in Atmospheric Studies Evaluation Number 15, JPL Publication, 06-2, 1–522, 2006.

Saunders, S. M., Jenkin, M. E., Derwent, R. G., and Pilling, M. J., Protocol for the development of the Master Chemical Mechanism, MCM v3 (Part A): tropospheric degradation of non-aromatic volatile organic compounds, Atmos. Chem. Phys., 3, 161–180, 2003, http://www.atmos-chem-phys.net/3/161/2003/.

Shirley, T. R., Brune, W. H., Ren, X., Mao, J., Lesher, R., Cardenas, B., Volkamer, R., Molina, L. T., Molina, M. J., Lamb, B., Velasco, E., Jobson, T., and Alexander, M.: Atmospheric oxidation in the Mexico City Metropolitan Area (MCMA) during April 2003, Atmos. Chem. Phys., 6, 2753–2765, 2006, http://www.atmos-chem-phys.net/6/2753/2006/.

Singh, H. B., Kanakidou, M, Crutzen, P. J., and Jacob, D. J.: High-Concentrations and Photochemical Fate of Oxygenated Hydrocarbons in the Global Troposphere, Nat., 378, 50–54, doi:10.1038/378050a0, 1995.

Stemmler, K., Ammann, M., Donders, C., Kleffmann, J., and George, C.: Photosensitized reduction of nitrogen dioxide on humic acid as a source of nitrous acid, Nat., 440, 195–198, doi:10.1038/nature04603, 2006.

Stutz, J., Alicke, B., Ackermann, R., Geyer, A., Wang, S. H., White, A. B., Williams, E. J., Spicer, C. W. and Fast, J. D.: Relative humidity dependence of HONO chemistry in urban areas, J. Geophys. Res.-Atmos., 109, D03307, doi:10.1029/2003JD004135, 2004.

Stutz, J., Kim, E. S., Platt, U., Bruno, P., Perrino, C., and Febo, A.: UV-visible absorption cross

sections of nitrous acid, J. Geophys. Res.-Atmos., 105, 14 585–14 592, doi:2000JD900003, 2000.
Vandaele, A. C., Simon, P. C., Guilmot, J. M., Carleer, M., and Colin, R.: SO2 absorption cross section measurement in the UV using fourier transform spectrometer, J. Geophys. Res., 99, 25599–25605, 1994.
Velasco, E., Lamb, B., Westberg, H., Allwine, E., Sosa-Iglesias, G., Arriaga-Colina, J. L., Jobson, T., Alexander, M., Prezeller, P., Knighton, B., Rogers, T. M., Grutter, M., Herndon, S., Kolb, C. E., Zavala, M. A., de Foy, B., Volkamer, R., Molina, L. T., and Molina, M. J.: Distribution, magnitudes, reactivities, ratios and diurnal patterns of volatile organic compounds in the Valley of Mexico during the MCMA 2002 & 2003 field campaigns, Atmos. Chem. Phys., 7, 329–353, 2007, http://www.atmos-chem-phys.net/7/329/2007/.
Volkamer, R., Etzkorn, T., Geyer, A., and Platt, U.: Correction of the oxygen interference with UV spectroscopic (DOAS) measurements of monocyclic aromatic hydrocarbons in the atmosphere, Atmos. Environ., 32, 3731–3747, doi:10.1016/S1352-2310(98)00095-8, 1998.
Volkamer, R., Platt, U., and Wirtz, K.: Primary and Secondary Glyoxal Formation from Aromatics: Experimental Evidence for the Bicycloalkyl-Radical Pathway from Benzene, Toluene, and p-Xylene, J. Phys. Chem. A, 105, 7865–7874, doi:10.1021/jp010152w, 2001.
Volkamer, R., Molina, L. T., Molina, M. J., Shirley, T., and Brune, W. H.: DOAS measurement of glyoxal as an indicator for fast VOC chemistry in urban air, Geophys. Res. Lett., 32, L08806, doi:10.1029/2005GL022616, 2005a.
Volkamer, R., Spietz, P., Burrows, J. P., and Platt, U.: High-resolution absorption cross-section of Glyoxal in the UV/vis and IR spectral ranges, J. Photochem. Photobio. A: Chem., 172, 35–46, doi:10.1016/j.jphotochem.2004.11.011, 2005b.
Volkamer, R., Jimenez, J. L., San Martini, F., Dzepina, K., Zhang, Q., Salcedo, D., Molina, L. T., Worsnop, D. R., and Molina, M. J.: Secondary organic aerosol formation from anthropogenic air pollution: Rapid and higher than expected, Geophys. Res. Lett., 33, L17811, doi:10.1029/2006GL026899, 2006.
von Friedeburg, C., Wagner, T., Geyer, A., Kaiser, N., Vogel, B., Vogel, H., and Platt, U.: Derivation of tropospheric NO3 profiles using off-axis differential optical absorption spectroscopy measurements during sunrise and comparison with simulations, J. Geophys. Res.-Atmos., 107, 4168, doi:10.1029/2001JD000481, 2002.
Wall, K. J., Schiller, C. L., and Harris, G. W.: Measurements of the HONO photodissociation

constant, J. Atmos. Chem., 55, 31–54, doi:10.1007/s10874-006-9021-2, 2006.
West, J. J., Zavala, M. A., Molina, L. T., Molina, M. J., San Martini, F., Mcrae, G. J., Sosa-Iglesias, G., and Arriaga-Colina, J. L.: Modeling ozone photochemistry and evaluation of hydrocarbon emissions in the Mexico City metropolitan area, J. Geophys. Res.-Atmos., 109, D19312, doi:10.1029/2004JD004614, 2004.
Zavala, M., Herndon, S. C., Slott, R. S., Dunlea, E. J., Marr, L. C., Shorter, J. H., Zahniser, M., Knighton, W. B., Rogers, T. M., Kolb, C. E., Molina, L. T., and Molina, M. J.: Characterization of on-road vehicle emissions in the Mexico City Metropolitan Area using a mobile laboratory in chase and fleet average measurement modes during the MCMA-2003 field campaign, Atmos. Chem. Phys., 6, 5129–5142, 2006, http://www.atmos-chem-phys.net/6/5129/2006/.
Zhou, X. L., Civerolo, K., Dai, H. P., Huang, G., Schwab, J., and Demerjian, K.: Summertime nitrous acid chemistry in the atmospheric boundary layer at a rural site in New York State, J. Geophys. Res.-Atmos., 107, 4590, doi:10.1029/2001JD001539, 2002.

Table 1. The percentage contributions of individual sources to OH_{new}.

		% contribution to ΣOH_{new}								
		03:00	07:00	09:00	11:00	13:00	15:00	20:00	06–18 (avg)	20–04 (avg)
Measured	HONO	––	45.6	24.2	8.0	4.0	1.2	––	12.8	––
	PSS [a]	––	*53-98*	*91-99*	*45-86*	*53-92*	*50-94*	––	*80-90*	––
	Dark + other [a]	––	*≤ 47*	*≤ 9*	*≤ 55*	*≤ 47*	*≤ 50*	––	*≤ 20*	––
	O_3	––	––	4.5	23.4	38.2	31.6	––	20.8	––
	HCHO	––	4.7	22.6	25.4	22.1	19.7	––	21.1	––
	Primary [b]	––	*60.5*	*40.0*	*11.9*	*0.1*	*6.2*	––	*28.6*	––
	Other [b]	––	*39.5*	*60.0*	*88.1*	*99.9*	*93.8*	––	*71.4*	––
	CH_3CHO	––	0.2	1.1	1.7	2.2	3.1	––	1.7	––
	CHOCHO	––	0.1	0.7	1.0	1.1	0.8	––	0.9	––
	CH_3COCH_3	––	0.06	0.22	0.28	0.47	0.42	––	0.32	––
	O_3 + alkenes	82.3	24.6	19.1	10.6	4.7	12.1	79.5	13.6	85.2
	→ *OH* [c]	*55.5*	*48.2*	*50.4*	*52.4*	*52.5*	*53.0*	*55.0*	*51.6*	*53.3*
	→ *HO_2* [c]	*8.2*	*6.6*	*8.8*	*11.7*	*12.2*	*11.3*	*9.6*	*10.0*	*8.1*
	→ *RO_2* [c]	*36.3*	*45.2*	*40.8*	*35.8*	*35.2*	*35.7*	*35.4*	*38.4*	*38.6*
Modeled	other OVOC	––	21.5	26.1	27.0	24.4	26.1	––	26.8	––
	→ *HO_2* [c]	––	*50.7*	*55.5*	*60.2*	*61.3*	*62.1*	––	*57.3*	––
	→ *RO_2* [c]	––	*49.3*	*44.5*	*39.8*	*38.7*	*37.9*	––	*42.7*	––
	NO_3 + VOC	17.7	0.2	1.1	2.1	1.8	3.6	20.5	2.2	14.8
	ROOH	––	––	0.1	0.2	0.8	1.3	––	0.4	––
	Sum	100.0	97.1	99.7	99.7	99.8	99.9	100.0	97.9	100.0

[a] PSS: photostationary state HONO; dark + other: unaccounted HONO sources. Numbers indicate relative contributions to OHnew production from HONO; [b] Primary: emission-related HCHO; other: photochemical and background HCHO (Garcia et al., 2006). Numbers indicate relative contributions to OHnew production from HCHO; [c] Numbers indicate relative contributions to OHnew production.

Table 2. Comparison of the relative importance of radical sources in Mexico City with other urban and rural atmospheres (daytime average HO_x radical production rates).

	HCHO Phot.	HONO Phot.	O_3 Phot.	O_3/ alkenes	others	References
Rural boundary layer						
Pinnacle State Park, NY, USA	14	18	44	n.n.	25[a]	(Zhou et al., 2002)
Forest near Julich, GER	25	27	23	6	20[a]	(Kleffmann et al., 2005)
Hohenpreissenberg, GER	14	32	30	n.n.	25[a]	(Acker et al., 2006)
Urban boundary layer						
Milan, Italy	34	16	20	8	20[a]	(Alicke et al., 2002)
Nashville, TN, USA	29	8	47	0.2	20[a]	(Martinez et al., 2003)
Pabstum (near Berlin), GER	37	17	39	6	2[b]	(Alicke et al., 2003)
New York City, NY, USA	8	56	13	10	13[c]	(Ren et al., 2003)
Birmingham, UK (summer)	8	7	6	25	54[d]	(Emmerson et al., 2005)
Birmingham, UK (winter)	1	15	0.5	59	26[d]	(Emmerson et al., 2005)
Chelmsford (near London), UK	6	10	14	20	50[d]	(Emmerson et al., 2007)
Mexico City, MEX	21	13	21	14	31[d]	This work

[a] no number; value assumed for normalization and comparison purposes.
[b] only selected carbonyls measured; lower limit number.
[c] estimated using RACM.
[d] estimated using MCMv3.1 (mostly photolysis of OVOC).

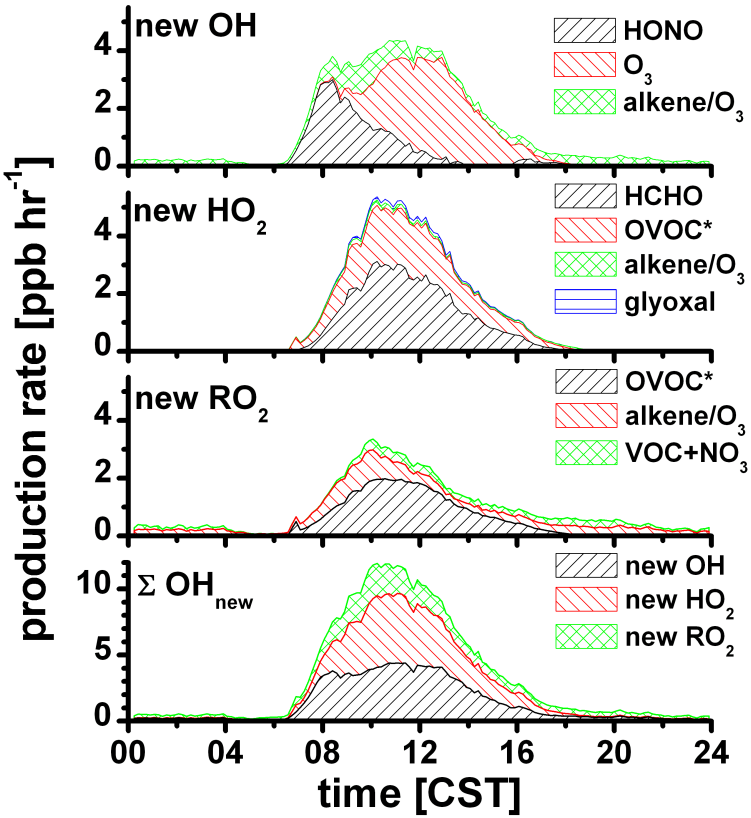

Fig. 1. Diurnal profiles of new RO_x radical formation from different sources. The categories marked with a star (*) indicate that the reactants are not constrained by measurements. The bottom graph shows the contribution of each RO_x species to ΣOH_{new}, accounting for their respective conversion factors.

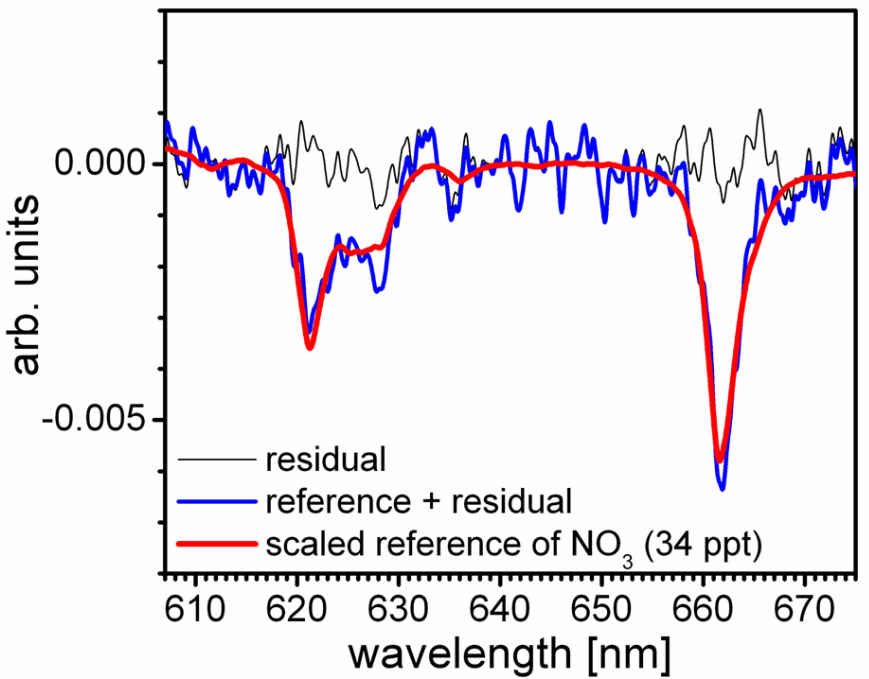

Fig. 2. Spectral proof for the detection of NO_3 radicals in Mexico City (29 April 2003, 01:17 a.m. CST). The atmospheric spectrum (blue line) has been corrected for NO2, and water absorptions, and shown with an accordingly scaled NO_3-reference spectrum (red line) from our previous work.

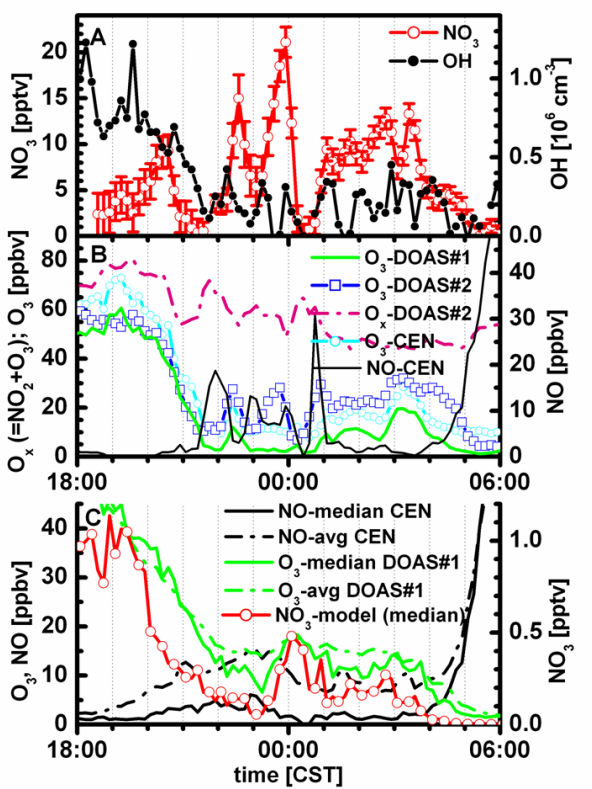

Fig. 3. Nighttime concentration-time profiles of NO_3 radicals and OH radicals during the night from 25 to 26 April 2003 (panel **A**), O_3 (from two LP-DOAS and a point sensor), O_x (sum of O_3 and NO_2) and NO (panel **B**). Panel C compares average and median nighttime O_3 and NO concentrations, and shows NO_3-radical predictions from the median model. The nighttime OH-concentration tends to follow the time trace of O_3 better than that of NO_3 radicals.

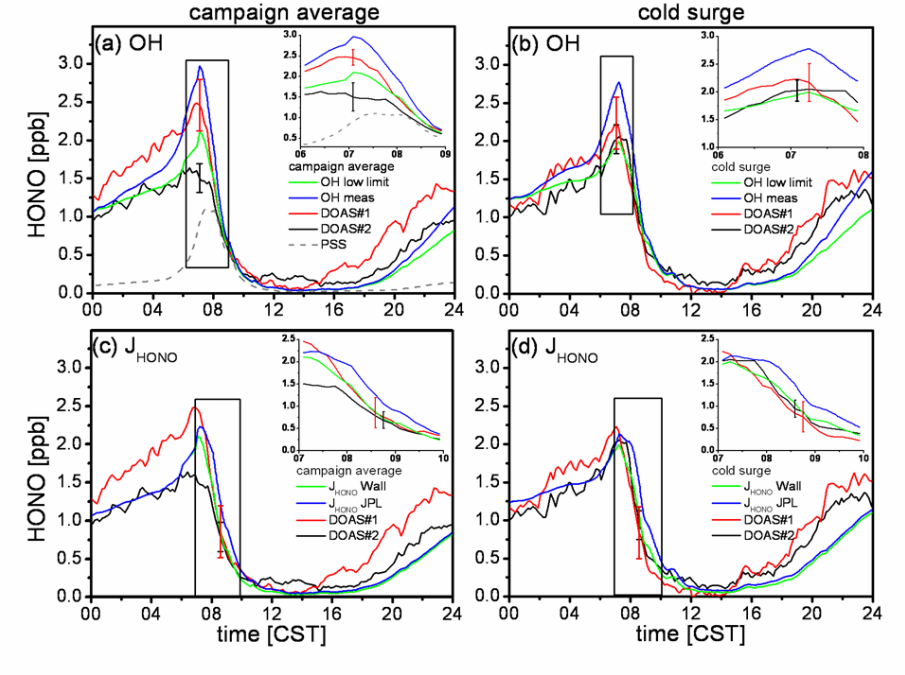

Fig. 4. Measured (red, black) and steady-state calculated (green, blue) values of HONO are shown for campaign-averaged data **(a, c)** and data averaged over cold-surge events **(b, d)**. The top two graphs show the modeled improvement when using a lower limit of OH. The bottom two graphs show the modeled improvement when using a higher value of JHONO, as recommended by Wall et al. (2006). The agreement between measured and modeled HONO concentrations suggests that HONO is a radical reservoir, rather than a source, in the MCMA, and presents independent evidence for faster-than-expected HONO photolysis.

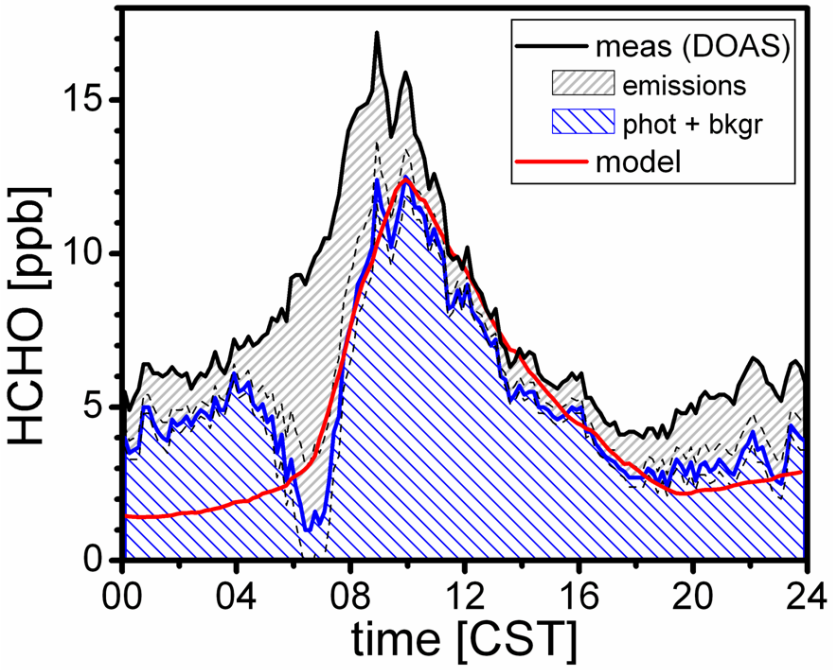

Fig. 5. HCHO observations (black line) are compared to the portion of HCHO produced from photochemical sources and background sources (blue line, shaded blue area), and from emissions (shaded gray area); the dotted lines represent the upper and lower limits of subtracting out emissions sources according to the procedure described by (Garcia et al., 2006). Modeled HCHO concentrations (red line) are shown in which dilution was adjusted to match the blue line (after 10:00 a.m., see Sect. 2.2).

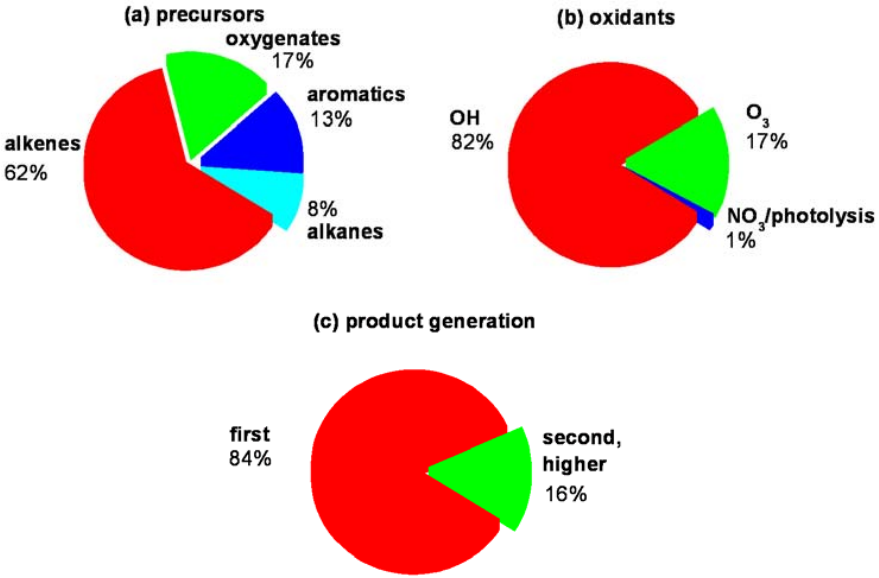

Fig. 6. Source apportionment of photochemical HCHO production. **(a)** The precursors of HCHO are separated by VOC class. **(b)** The effect of different oxidants is assessed. **(c)** The time scale of HCHO production is assessed in terms of oxidation step. An overwhelming majority of HCHO is formed as a first generation oxidation product from VOC oxidation; HCHO formation as second- and higher generation oxidation products makes only a minor contribution.

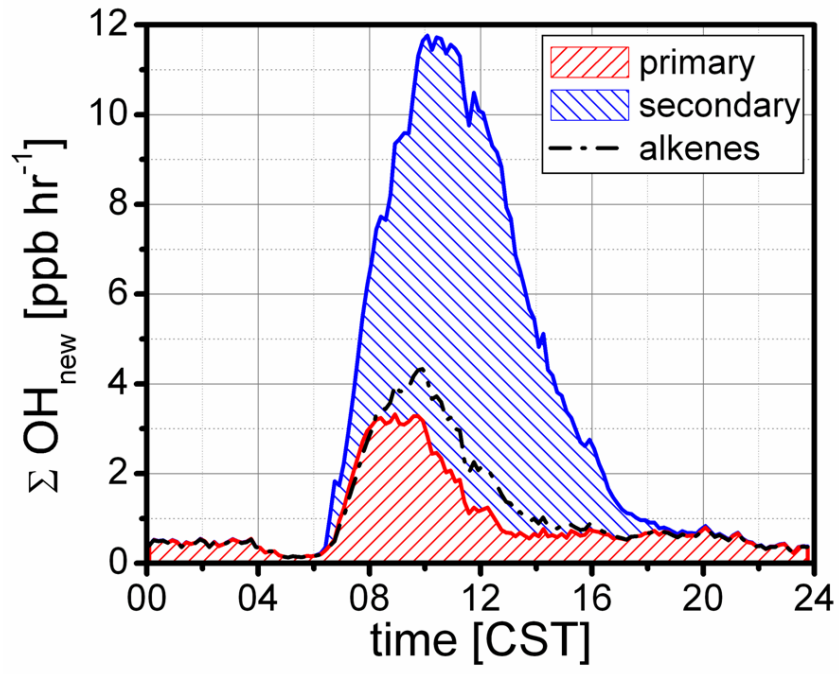

Fig. 7. The OH-equivalent radical production rate grouped by primary (emission related) vs. secondary (photochemistry related) sources. Primary sources are taken as the sum of O_3/alkenes, primary HCHO, the portion of PSS-HONO formed from primary radical sources, and alkene/NO_3 reactions. Secondary sources are taken as the photolysis of O_3, other HCHO, other OVOCs, the portion of PSS-HONO formed from secondary radical sources, unaccounted HONO, and further NO_3 reactions. The dashed-dot line represents a lower limit of the sum of primary and secondary OHnew production attributable to alkenes.